American Journal of Environmental Policy and Management
2018; 4(1): 21-31
http://www.aascit.org/journal/ajepm
ISSN: 2472-971X (Print); ISSN: 2472-9728 (Online)

American Association for Science and Technology

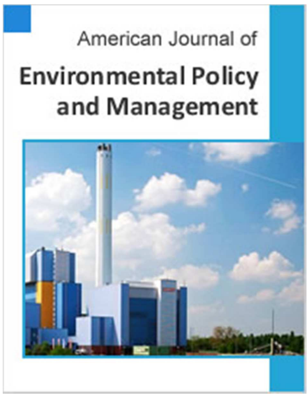

Keywords
Vegetation Fractional Coverage,
NDVI,
Spatial-Temporal Dynamics,
Driving Factors

Received: August 23, 2017
Accepted: December 9, 2017
Published: January 18, 2018

Vegetation Fractional Coverage (VFC) Estimation of Planted and Natural Zones Based on Remote Sensing

Seyed Omid Reza Shobairi[1, *], Vladimir Andreevich Usoltsev[1, 2], Viktor Petrovich Chasovskikh[1]

[1]Department of Forest and Environmental Sciences, Ural State Forest Engineering University, Yekaterinburg, Russian Federation
[2]Ekaterinburg Botanic Garden, Yekaterinburg, Russian Federation

Email address
Omidshobeyri214@gmail.com (S. O. R. Shobairi)
[*]Corresponding author

Citation
Seyed Omid Reza Shobairi, Vladimir Andreevich Usoltsev, Viktor Petrovich Chasovskikh. Vegetation Fractional Coverage (VFC) Estimation of Planted and Natural Zones Based on Remote Sensing. *American Journal of Environmental Policy and Management*. Vol. 4, No. 1, 2018, pp. 21-31.

Abstract
In the field of remote sensing, an important index likewise vegetation fractional coverage (VFC) is widely used to monitor condition of the all plant communities that cover the Earth's surface. This paper selected two phase of remote sensing data calculation such as normalized difference vegetation index (which extracted from cloud-free Modis NDVI) to derive vegetation fractional coverage, And compounded night light index (CNLI) from meteorological satellite program/operational line-scan system (DMSP/OLS) to measure human activity with more clarity. VFC were classified in four levels and spatial patterns of VFC changes were accordingly derived with different coverage at a research period of 16 years (2000-2015). Finally this process led to forecast time series analysis of VFC. Another calculation has been made clear that the driving factors of VFC dynamics were considered to various factors such as human activities, environmental and climatic factors, etc. The correlation coefficient confirmed the relationship between urbanization indexes (CNLI), population, environmental and climatic factors which is linked to VFC. Finally, driving factors of VFC dynamics have been influenced by climatic factors likewise rainfall (mm) and temperature (°C), although the impact of human factors has been impressive.

1. Introduction

Science of the vegetation coverage structure is important for understanding interactions among terrestrial ecosystems (Colombo et al., 2003; Ju et al., 2013; Hyung, 2014). Vegetation, including forests, bushes, grasslands, farmlands, and orchards, as important components of the ecological cycle, can maintain the ecological environment (Zhang et al., 2013; Guan et al., 2013), so that it has been especially considerable in the last few decades. The vegetation fractional coverage (VFC), which represents the horizontal density of live vegetation, is of particular importance for regional and global carbon modeling, ecological assessment, and agricultural monitoring (Asner and Lobell, 2000; Lucht et al., 2002). VFC includes some vertical projection of vegetation such as leaves, stem and shoots (Wu et al., 2014). VFC changes due to land use-land cover changes increased, and other side monitoring of VFC has a necessary significant for global energy cycle and geo-biochemical circulation of substance (Yang et al., 2010). Among many forest structure variables, vegetation fractional cover, defined as the fractional area (projected vertically) of vegetation canopy occupying a given land area (Li et al., 2009), is a key parameter for modeling the exchanges of carbon on the land surface and for monitoring urban environment and urban growth (Potter et al., 2008; Kouchi et al., 2013). However, it is very important to predict the dynamic of global VFC with the field sampling, GIS special analysis, artificial neural network (ANN) and especially calculation of satellites products as NDVI (normalized different vegetation index) (Potapov et al., 2015; Jiapear et al., 2011). Methods of calculating the VFC by spatial resolution, spectral resolution and temporal resolution of imagery that got on a different remotely sensed platforms or different sensors are dissimilar (Chen et al., 2001). According to scope of imagery, the satellite remotely sensed data can reflect the detail changes from local to global scale. Some methods using remotely sensed data to predict the vegetation fractional coverage have been included experiential model, vegetation index and sub-pixel decomposition (Chen et al., 2001; Hao et al., 2003; Kouchi et al., 2013). Thus, choosing proper vegetation index is significant to predict the vegetation fractional coverage. According to different demands, the appropriate sensor was selected as various modes to simulate the vegetation fractional coverage. The result measured by remote sensing data must be verified by field survey data. Recent studies have shown that hyperspectral data enables to eliminate the scattering effect of soil and atmosphere on sensor reflectance (Estel et al., 2015). In addition, it can reflect the direct chlorophyll concentration and leaf area index and develop the accuracy of vegetation fractional coverage predicted by remotely sensed data (Kenneth et al., 2000). On the other side, simulating the vegetation fractional coverage using multi-scale remotely sensed data such as MODIS doesn't enable to meet different requirements to ground surface parameters of model, however to improve the accuracy of measurement on large scale, it is one of important methods of scaling research using remote sensing data (Hao et al., 2003; Schneider et al., 2009; Burges et al., 2012). Effective monitoring of VFC requires longer-term data set with fine spatial resolution-ideally at sub-hectare spatial resolutions spanning multiple decades (Sexton et al., 2013). In this context, satellite borne sensors can detect VFC change in the visible, thermal and mid-infrared signature during the days, nights, months and seasons (Chand et al., 2006). In this study, we are going to use one of the most common satellite systems as MODIS (Moderate Resolution Imaging Spectroradiometer) from NASA which provides visible and thermal images and also it can be evaluated vegetation cover changes. There are a lot of projects that were defined start and end of the growing season using MODIS-based 16-days NDVI profiles derived within MODIS-based forest cover mask (Potapov et al., 2015). The growing season was defined as the sum of all 16-day intervals having an NDVI equal to or above 90% of the maximum annual NDVI. NDVI is considered as a simple graphical indicator that can be used to analyze remote sensing measurements, typically but not necessarily from a space platform, and assess whether the target being observed contains live green vegetation or not. For example, negative values of NDVI (values approaching -1) correspond to water. Values close to zero (-0.1 to 0.1) generally correspond to barren areas of rock, sand, or snow. Lastly, low, positive values represent shrub and grassland (approximately 0.2 to 0.4), while high values indicate temperate and tropical rainforests (values approaching 1). The NDVI images of MODIS (1 month-Terra) from the NEO (Nasa Earth Observations) data archive can be used as based datasets (http://modis.gsfc.nasa.gov/). Using NDVI images are directly computed VFC and as it was mentioned above, VFC is the vertical projection of vegetation including leaves, stems, and also shoots to the ground surface and is expressed as the fraction or percentage of the reference area (Zhang et al., 2013). In fact, VFC enables to couple natural environment changes and human activities and also it is an essential index to study the ecological systems (Liu et al., 2009). In addition, vegetation changes attaches a great importance to global energy circulation and geo-biochemical cycle of substance, thus evaluating VFC contains a great significant for both ecology system and society (Ju et al., 2013). On the other side we applied DMSP/OLS night time lights data series to calculate CNLI. CNLI is considered as one of the most significant driving forces on VFC dynamics. In fact, visible and infrared imagery from DMSP/OLS instruments are used to monitor the global distribution of clouds and cloud top temperatures twice each day. The archive data set consists of low resolution global and high resolution regional, imagery recorded along a 3,000 km scan, satellite ephemeris and solar and lunar information. Infrared pixel values correspond to a temperature range of 190 to 310 Kelvins in 256 equally spaced steps. Onboard calibration is performed during each scan. Visible pixels are relative values ranging from 0 to 63 rather than absolute values in Watts per m^2. Instrumental gain levels are adjusted to maintain constant cloud reference values under varying conditions of solar and lunar illumination. Telescope pixel values are replaced by Photo Multiplier Tube (PMT) values at night. A telescope pixel is 0.55 km at high resolution (fine mode) and 2.7 km at low resolution (smooth mode). Low resolution values are the mean of the appropriate 25 high resolution values. DMSP/OLS data enables us to makes daily over-flights and routinely collects visible images during its nighttime pass (Kharol et al., 2008). In fact, measured DMSP/OLS data is possible to detect human presence, urban people, settlements and light-demanding activities, energy, electricity consumption and gas emissions (Amaral et al., 2006; Huang et al., 2014).

The main objective of this research is to analyze the dynamic of VFC, classification of VFC, time series analysis of VFC, trend analysis of VFC, time series trend of VFC and finally computation of driving factors of VFC dynamics such as human activity and climatic factors during the years of 2000 to 2015.

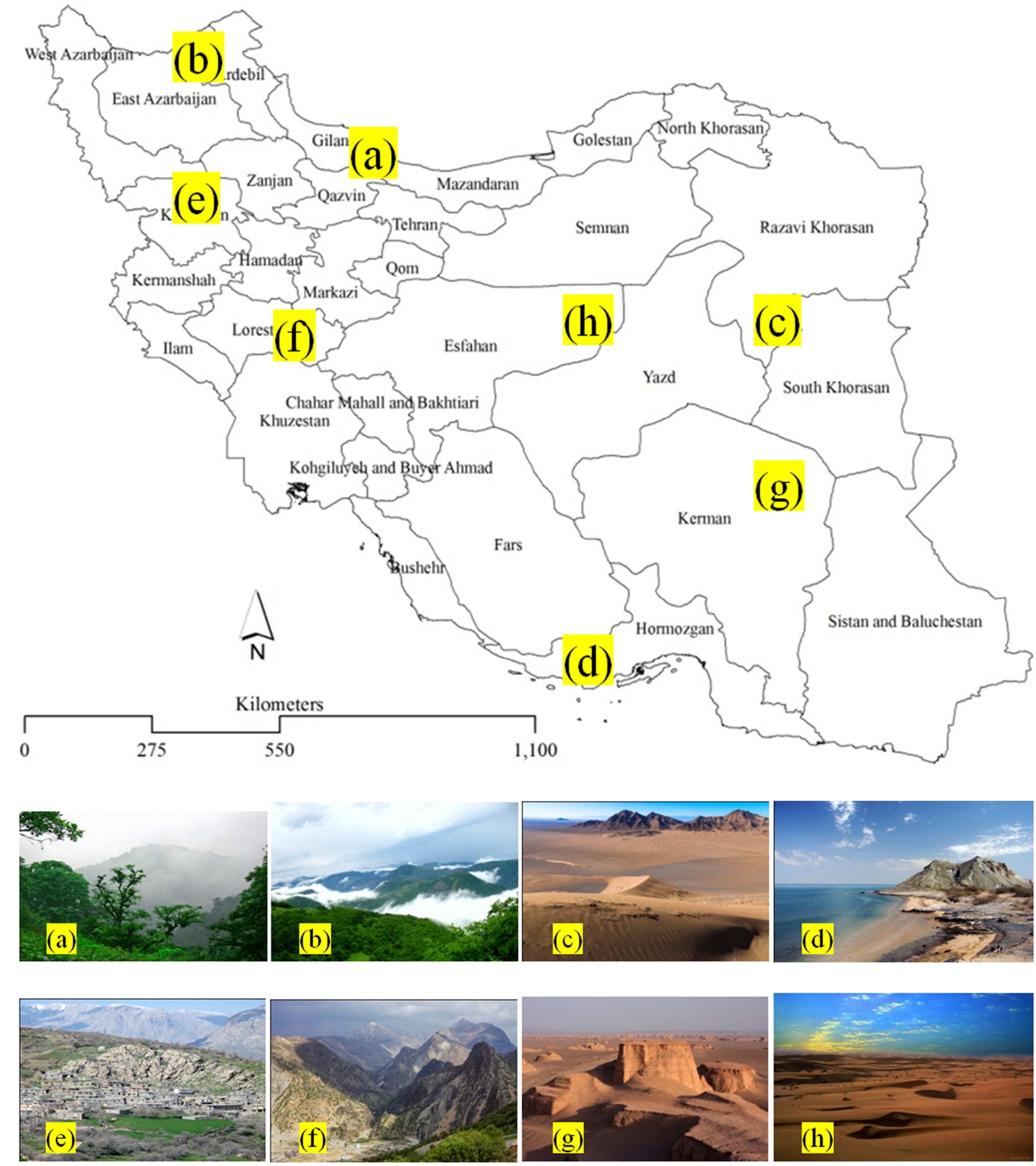

Figure 1. Geographical location along with provinces and regions, Iran.

2. Materials and Methodology

2.1. Study Area

Iran lies between latitudes 24° and 40° N, and longitudes 44° and 64° E. Figure 1 shows the map of Iran with geographical collation of province boundary. Iran is a sovereign state in Western Asia, comprising a land area of 1,648,195 km^2; it is the second-largest country in the Middle East and the 18th-largest in the world, and a population of about 79.2 million people in 2016; was one of the growing populated areas in the world. Studies project that the growth will continue to slow until it stabilizes above 105 million by 2050. At present, Iran is the world's 17th-most-populous country. The northern part of Iran is known coastal region of the Caspian Sea that covered by dense rain forests (Hyrcanian[1] and Arasbaran[2]). The eastern part and central portion consists mostly of desert basin, as well as deserts and salt lakes that most famous are Dasht-e Kavir and Dasht-e Lut. West part occupies by the largest mountains range (Zagros[3]) and Persian oak forest and other species cover more than half of the mentioned regions. south part of Iran are along the remaining coast of the Persian Gulf, the Strait of Hormuz and the Gulf of Oman, that can be observed Mangrove forest in some areas exclusively. Iran's climate ranges from arid or semiarid, to subtropical along the Caspian coast and the northern forests. On the northern edge of the country temperatures rarely fall below freezing and the area remains humid for the rest of the year. Summer temperatures rarely exceed 29°C. Annual precipitation is 680 mm in the eastern part of the plain and more than 1,700 mm in the western part. To the west, settlements in the Zagros basin experience lower temperatures, severe winters with below zero average daily temperatures and heavy snowfall. The eastern and central basins are arid, with less than 200 mm of rain, and have occasional deserts. Average summer temperatures rarely exceed 38°C. The coastal plains of the Persian Gulf and Gulf of Oman in southern Iran have mild winters, and very humid and hot summers. The annual precipitation ranges from 135 to 355 mm.

2.2. Datasets

2.2.1. NDVI Data

The NDVI datasets with minimizing phonological and atmospheric noise extracted from the website of NEO datasets (http://neo.sci.gsfc.nasa.gov/), by appropriate based on phonological time series of vegetation index from the MODIS. The desired data selected from the start and end of the growing season from April to October during the years 2000 to 2015. MODIS plays a vital role in the development of validated, global, interactive earth system models able to predict global change accurately enough to assists policy makers in making sound decisions concerning the protection of our environment (Lyapustin et al., 2014).

2.2.2. DMSP/OLS Data

The night time lights datasets derived DMSP/OLS satellites such as F14, F15, F16 F18 by years 2000 to 2015 in sun synchronous orbits with nighttime overpasses ranging from nearly 8 pm to 10 pm local time. Elvidge et al. (2009) concluded the time series of DMSP/OLS nighttime lights for the period of 2000-2010 were collected by individual sensors: F14 (1997-2003), F15 (2000-2007), F16 (2004-2009) and F18 (2010-2015). The DMSP/OLD data were obtained from the web site of NOAA (http://www.ngdc.noaa.gov/ngdc.html) directly. Given the sensitivity of the sensor at night, DMSP/OLS data can be used to detect a variety of VNIR emissions (Small et al., 2005). The availability of long time data with moderate spatial resolution (e.g., 1 km) has enabled researchers to explore a series of global, national and regional research subjects (Elvidge et al., 2009; He et al., 2015). In present paper, DMSP/OLS nighttime data use to directly calculate CNLI and to evaluate human activities such as urbanization and other socio-economic activities (Huang et al., 2014).

2.2.3. Climatic Data

Two climatic data datasets were compared to investigate their influence on VFC calculations. One was the mean of rainfall (mm), and the other was mean of temperature (°C), which both were considered an annual report from 2000 to 2015. The mentioned data were derived from the website of Climate Change Knowledge Portal (CCKP) (http://sdwebx.worldbank.org/climateportal.html).

---

1 Hyrcanian forest granted the areas with unique richness of biological diversity, its endemic and endangered species, its natural beauty and its masterpieces of nature creative genius in the form of this ancient forest. North of Iran as along band has diverse natural, economic and social conditions. It characterized by various ecological conditions from 550 to 2200 mm precipitation, zero to 5671 m elevation and various vegetation landscape from conifers to broadleaved to Mediterranean plants. These conditions caused great diversity in species. It due to its diverse ecological condition is rich in relict species that some of them referred to the Tertiary period. Hyrcanian forest contain the most important and significant natural habitats for in-situ conservation of biological diversity, including those containing threatened species of outstanding universal value from the point of view of science or conservation. It also contains superlative natural phenomena or areas of exceptional natural beauty and aesthetic importance. It is outstanding examples in the record of significant on-going geological processes in the development of landforms and significant geomorphic or physiographic features. It is also outstanding example representing significant ongoing ecological and biological processes in the evolution and development of terrestrial, ecosystems and communities of plants.

2 The Arasbaran biosphere reserve is situated in the north of Iran at the border with Armenia and Azerbaijan in the Caucasus Iranian Highlands. The reserve encompasses mountains, high alpine meadows, semi-arid steppes, rangelands and forests, rivers and springs. Arasbaran is a high mountainous region with an elevation ranging from 256 m to 2,896 m above sea level. The area encompasses part of the Caucasus mountains with diverse natural landscapes including highlands, steep valleys, high and steep mountain sides, forest lands, and agricultural, mountainous and river rangelands. The Arasbaran vegetation is of particular importance among the vegetation of the country because of the uniqueness.

In general, there are 48 mammal species, 215 bird species, 29 creeper species, 5 amphibian species and 17 fish species occupying different habitats of the reserve. Over 1,000 plant species can be found in the reserve that survived the ice age and can be considered living fossils of the past.

3 The Zagros Mountains contain several ecosystems. Prominent among them are the forest and forest steppe areas with a semi-arid climate. As defined by the World Wildlife Fund and used in their Wild finder, the particular terrestrial ecoregion of the mid to high mountain area is Zagros Mountains forest steppe. The annual precipitation ranges from 400 mm to 800 mm (16 to 30 inches) and falls mostly in the winter spring. The winters are severe, with low temperatures often below -25 °C (-13 °F). The region exemplifies the continental variation of the Mediterranean climate pattern, with a snowy, cold winter and mild rainy spring followed by a dry summer and autumn. Although currently degraded through overgrazing and deforestation, the Zagros region is home to a rich and complex flora. Remnants of the originally widespread oak-dominated woodland can still be found, as can the park-like pistachio/almond steppelands. The ancestors of many familiar foods, including wheat, barley, lentil, almond, walnut, pistachio, apricot, plum, pomegranate and grape can be found growing wild throughout the mountains. Persian oak (*Quercus brantii* Lindl) (covering more than 50% of the Zagros forest area) is the most important tree species of the Zagros in Iran.

3. Methods

3.1. The formation of NDVI

NDVI captures the contrast between the visible-red and near-infrared reflectance of vegetation canopies, and is defined as:

$$NDVI = (NIR - RED)/(NIR + RED) \quad (1)$$

3.2. VFC Calculation Model

VFC calculated from 2000 to 2015. $NDVI_{min}$ is minimum of NDVI value and $NDVI_{max}$ is maximum of NDVI value. The VFC is calculated as follows;

$$VFC = \frac{NDVI - NDVImin}{NDVImax - NDVImin} \quad (2)$$

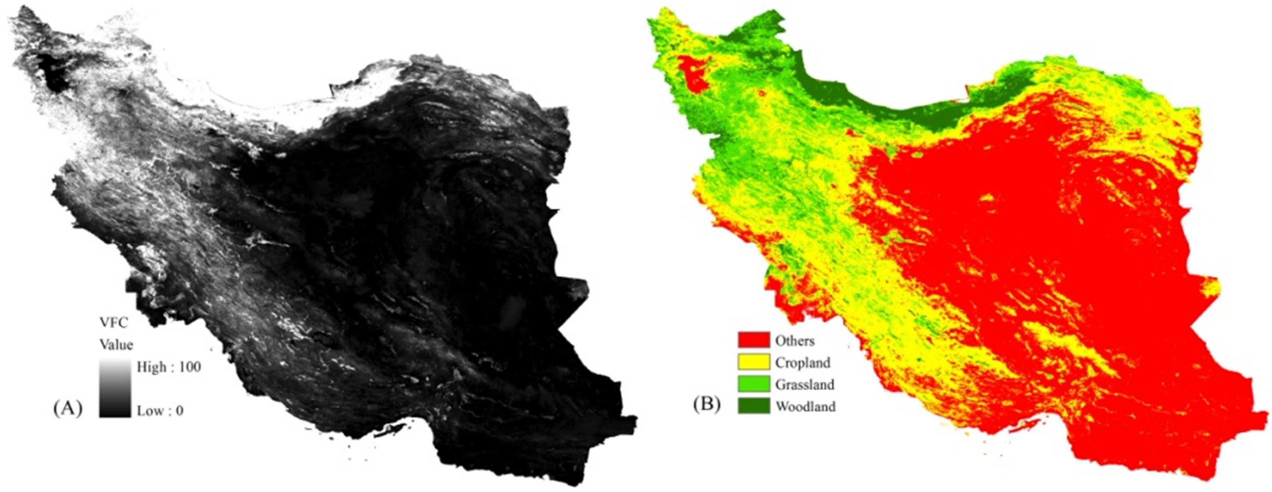

Figure 2. *Distribution of VFC values (A) and validation samples (B), based on Iran vegetation fractional coverage in 2012, at 30-m spatial resolution. The pre-processing techniques were applied to the NDVI data, including fixing bad and outlier pixels, local destriping, atmospheric correction, and minimum noise fraction smoothing, which ensures a consistent and standardized time series of data that is compatible with field-scale and airborne measured indices. To match them with validation samples, the VFC dynamic was calculated. The VFC was reclassified into 4 dominant categories.*

1) Class IV (Woodland); with very high vegetation coverage; VFC is more than 70%; this class includes dense woodland and northern hardwood forest.
2) Class III (Grassland); with high vegetation coverage; VFC is among 40% to 70%; this class includes semi-dense grassland, shrubland and oak forest.
3) Class II (Cropland); with medium vegetation coverage; VFC is among 10% to 40%; this class includes more farms, cropland, with low condensed plant community.
4) Class I (Others); with low, very low or non vegetation coverage; VFC is less than 10%; this class includes desert, insignificant plant community, barren land, sand, etc.

3.3. Time Series Analysis of VFC

Time series analysis calculated using annual VFC data from 2000 to 2015. Time series forecasting model of export computed to fit the annual VFC data.

3.4. Trend Analysis of VFC

Trend analysis using cubic polynomial with least root mean square error was calculated by spatial toolset of ArcGIS 9.3. VFC classified into four levels such as low (<10%), medium (10-40%), high (40-70%) and very high (>70%).

3.5. CNLI Determination and Validation

The importance of DMSP/OLS imageries has been explained (Figure 3). By DMSP/OLS data, CNLI computed at the scale of our study area using the following formula:

$$CNLI = I \times S \quad (3)$$

where I is the average night light brightness of all lit pixels in a region. It is illustrated as follows:

$$I = \frac{1}{N_L \times DN_M} \times \sum_{i=p}^{DN_M} (DN_i \times n_i) \quad (4)$$

where DN_i is the DN value of the ith gray level, n_i is the number of lit pixels belonging to the ith gray level, P is the optimal threshold to extract the lighted urban area from the DMSP/OLS images. DN_M is the maximum DN value, and N_L is the number of lit pixels with a DN value between P and DN_M. S is the proportion of lit urban areas to the total area of a region. It can be showed as follows:

$$S = \frac{Area_N}{Area} \quad (5)$$

where $Area_N$ is the area of lit urban areas in a region and $Area$ is the total area of the region.

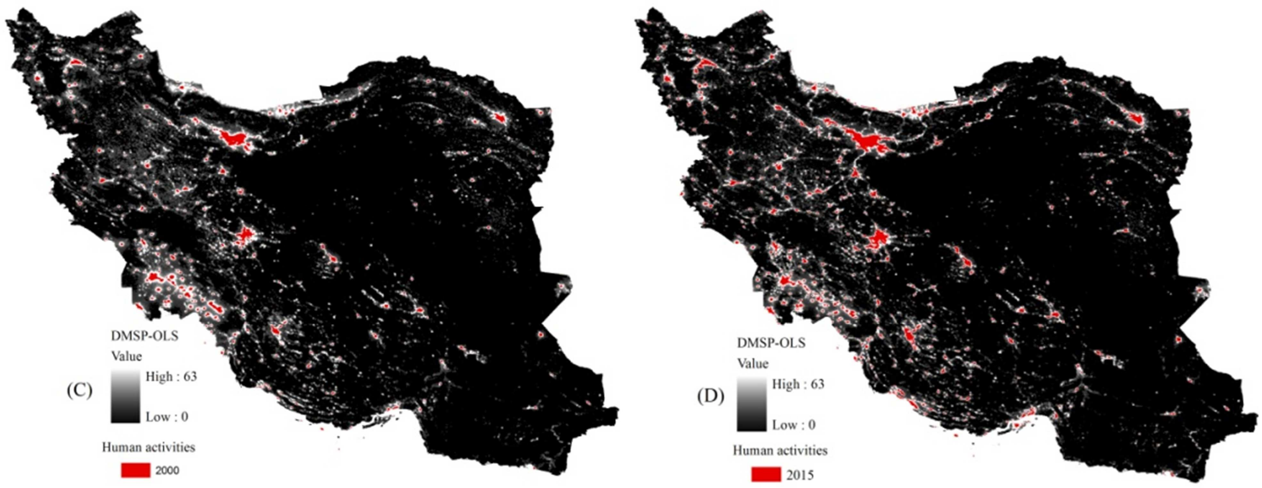

Figure 3. *DMSP/OLS night-time lights of Iran; Profile (C) and (D) are related to start and end of the study period, from 2000 to 2015 respectively. Since the CNLI helps to reflect the dynamics of urbanization levels, industrialization and population density at national scale, as well as Pearson correlation coefficient is used as a measure to assess the relationship among night-time lights index likewise CNLI with VFC during 16 years. (Cell size 30 arc second~1km², Iran boundary overlaid).*

3.6. Driving Forces Analysis of VFC Dynamics

Pearson correlation coefficient was confirmed to calculate the relationship between VFC, CNLI and climate factors eventually.

3.7. Time Series Trend of VFC

The time series trend of VFC dynamic of polygon themes for the entire period of 16 years overlaid in Arc View GIS and polygons of vegetation coverage change trend were mapped. Totally the technical flowchart of this research is as follows (Figure 4);

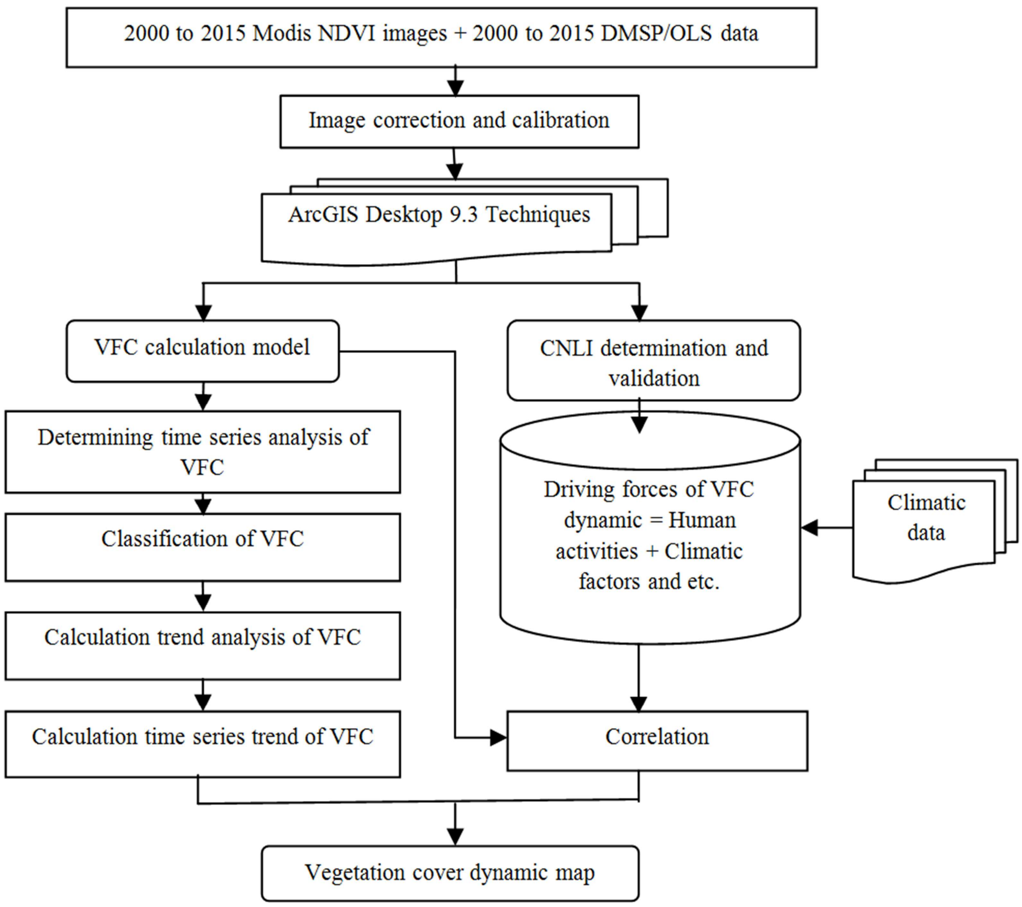

Figure 4. *Technical Flowchart.*

4. Results and Discussion

4.1. Time Series Analysis of VFC

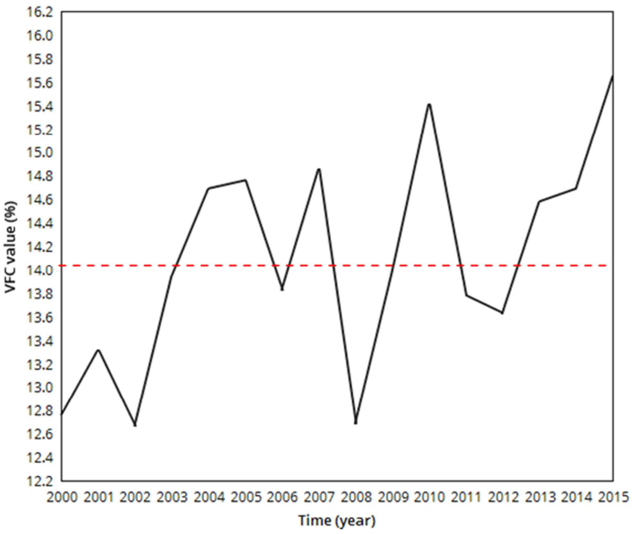

Figure 5. *Dynamics of VFC from 2000 to 2015.*

Time series analysis was done using annual VFC data from 2000 to 2015. Time series forecasting module of expert modeller was applied to fit the annual VFC data. An annual VFC curve and a fitting line were generated (Figure 5). As can be seen from Figure 5, the fitting curve is a straight line of value 0.1407 (14.07%) paralleling to the horizontal year axis. It should be noted that, during the period from 2000 to 2015, annual VFC fluctuated around the fitting straight line but showed no general trend of increase or decrease. Among sixteen research years, the VFC in 2003 and 2006 was equal to the average value of 14.07%, while the VFC in 2000, 2001, 2002, 2008, 2011 and 2012 was below the average and the remaining years above the average. According to the data provided by the Iran Meteorological Organization (http://www.irimo.ir/), some provinces were caught by a severe drought in 2000, 2001, 2002, 2007, 2008 and 2010. During these years, the precipitation was very sparse and rare, and the sunshine hour was very long, which not possible to promoted vegetation growth and resulting to decreasing annual VFC. On the contrary, in seven years from 2003, 2004, 2005, 2006, 2007, 2009 and 2013, there annually were average precipitation between 200 to 250 (mm) in Iran, causing a large area of crop and grass induced to grow, resulting in the increase of VFC.

4.2. Trend Analysis of VFC

VFC in four years from 2000, 2005, 2010 and 2015 were selected to do trend analysis using cubic polynomial with least RMSE supported by spatial analysis toolset of Arc GIS 9.3. Then VFC were classified into four categories: class I or low percent of VFC (<10%), class II or medium percent of VFC (10-40%), class III or high percent of VFC (40-70%) and class IV or very high percent of VFC (>70%). Finally, a VFC trend analysis map of VFC were produced (Figure 6).

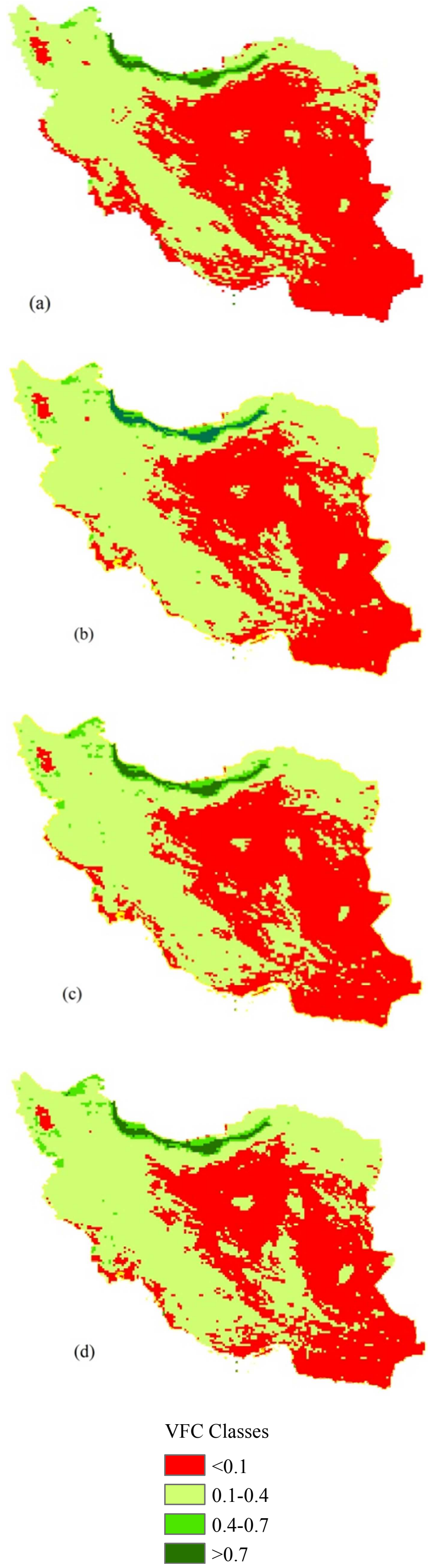

Figure 6. *Spatial trend dynamics of VFC from 2000 (a), 2005 (b), 2010 (c) and 2015 (d).*

The result of the evaluation of Figure 6 during the four periods of 2000, 2005, 2010 and 2015 explained as follow; 1) the spatial distribution of class I of VFC (<10%) is going down from the central parts to the south and southeast. 2) the class II of VFC (10-40%) has been increasing trend from the northwest parts to southwest and from west parts to the south, however it trend includes the parts of the northeast additionally. 3) the class III of VFC (40-70%) has been increased, so that this improvement has been mainly in the Hyrcanian and small parts of the northwest such as Arasbaran. in fact, this increase in class III is derived from land use changes of class IV of VFC to class III of VFC during the years of 2000 to 2005 and 2005 to 2010, however this class (class III) has been declining in 2010 to 2015 undoubtedly. 4) the spatial distribution of class IV of VFC (>70%) shows that this process has been a trend to increase at the beginning of the period and has been a trend to decline at the end of the period. Other change in vegetation coverage is visible by showing colored spatial distribution pattern (Figure 6).

As we discussed before, spatial pattern derived from DMSP/OLS night time lights imagery is closely related with regional differences in the level of industrialization and urbanization. The CNLI for the four mentioned categories during three periods of 2000, 2005, 2010 and 2015 were calculated 0.0406, 0.0397, 0.0633 and 0.0529 respectively. In the northwest and west mountainous regions of the study area, the economy is undeveloped and there is less human disturbance, resulting in the higher VFC, however this increase is also due to agricultural activities. In the north parts and southwest, especially in the Caspian delta region and Persian Gulf delta region human disturbance such as industrialization and urbanization is very strong, resulting in the low VFC.

Table 1. *Area change table of VFC of Guangdong in 2000, 2005, 2010 and 2015.*

Year	Low (<10%)	Medium (10-40%)	High (40-70%)	Very high (>70%)	VFC (%)	DMSP/OLS	CNLI
2000	55.52	41.74	1.37	1.34	1.34	2.56	0.0406
2005	51.56	45.23	1.78	1.41	1.32	2.45	0.0397
2010	47.61	48.72	2.27	1.39	1.41	2.69	0.0633
2015	43.24	53.13	2.25	1.37	1.29	2.08	0.0529

As can be seen from Table 1, during the four periods of 2000, 2005, 2010 and 2015, both the area ratio and spatial distribution pattern of different classes of VFC changed. From the viewpoint of area ratio, during 2000 to 2015, the percentage of medium and high class of VFC increased gradually, while the percentage of low class of VFC decreased. However, the percentage of very high VFC showed a more complex trend of a slight upward first (2000-2005), then decline (2005-2010-2015). Other changes based on four classes of VFC can be seen in Figure 7.

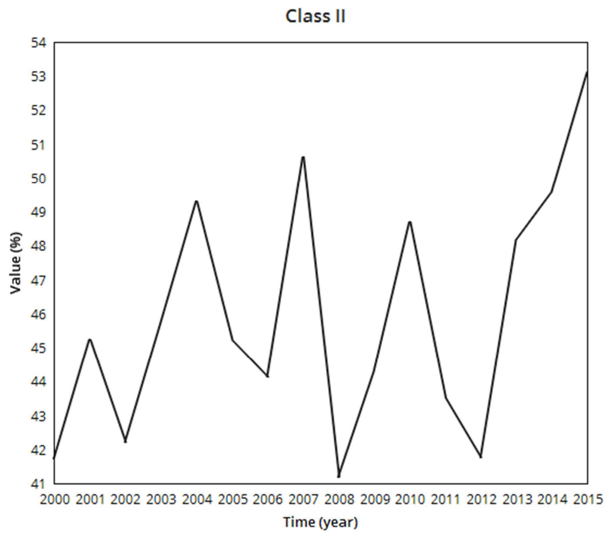

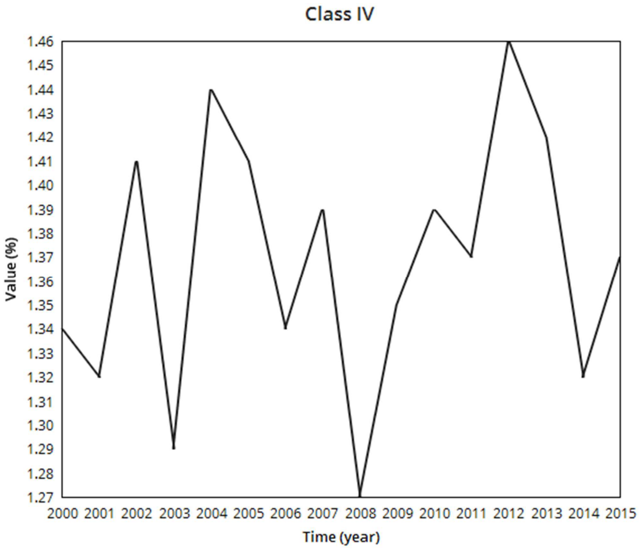

Figure 7. *Validation of the VFC calculation based on four different classes.*

4.3. Time Series Analysis Trend of VFC

The findings of time series analysis trend of VFC showed that VFC has been declining from coastal area of the Caspian Sea, some parts of central and northeast area. Even thought, the reduction process of VFC in the west and especially southwest region (Zagros) is visible during the sixteen year (Figure 8). In the following section be determined that the human activities such as industrialization, urbanization, and other driving forces likewise population, environmental and climatic factors will be mainly effective on the trend of VFC.

In return, VFC was rarely improved with more intensity in the west and northwest and additionally with low intensity in parts of the northeast and southeast; however the provinces with high and very high VFC gradually moved from west parts to the northwest that the trend of VFC has been increasing well. The most important result was that the area with the rich background of forest resources (Hyrcanian) was dramatically reduced in three distinct parts from 2000 to 2015 (Figure 8).

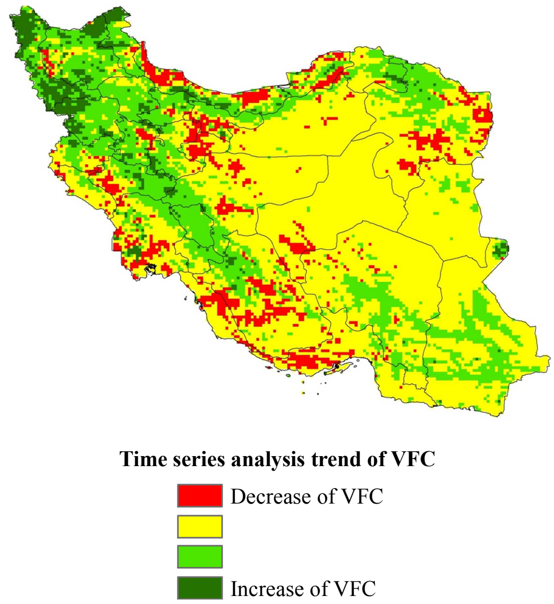

Figure 8. *Distribution changes of time series analysis trend of VFC.*

4.4. Driving Factors of VFV Dynamics

Totally it has been made clear that the driving factors of VFC dynamics were considered various factors such as human activities, environmental and climatic factors and etc. Pearson correlation coefficient was calculated to analyze the relationship between urbanization indexes (CNLI), population, environmental and climatic factors which is closed with VFC (Table 2). If the correlation coefficient is | r |> 0.90, there is a significant correlation between the two variables; if | r | ≥0.8, is highly relevant; if 0.5≤ | r | <0.8, is moderately correlated; if 0.3≤ | r | <0.5, there is 1 low correlation; if | r | <0.3, there is a very weak relationship between two variables.

Table 2. *Pearson correlation of VFC, climate factors and CNLI.*

	Mean of Rainfall (mm) Annually	**Mean of Temperature (°C) Annually**	**VFC**	**VFC %**	**DMSP-OLS**	**CNLI**	**CO_2 (Ton)**	**Population (million)**
Mean of Rainfall (mm) Annually	1							
Mean of Temperature (°C) Annually	-0.6104	1						
VFC	0.5691	0.5513	1					
VFC %	0.6379	0.4344	0.9598	1				
DMSP-OLS	-0.4300	0.2664	0.5509	0.5947	1			
CNLI	-0.4318	0.2693	0.5499	0.5930	0.9999	1		
CO_2 (Ton)	-0.1719	-0.0599	0.2905	0.3706	0.7912	0.7901	1	
Population (million)	-0.0187	-0.0746	0.3944	0.4758	0.7579	0.7570	0.9692	1

As showed from Table 2, VFC is positively correlated with mean of rainfall (mm), also VFC moderately correlated with mean of temperature annually. VFC is low correlated with population and CO_2 emission (Ton/Year). The reason why VFC is positively correlated with mean of temperature in the fact that number of sunny days is significant and it can promote plant photosynthesis and help to increase VFC. In some provinces, rain always appears in the form of scattered showers and incomplete rainfall which causes large area of farmland and grassland became facing with drought, leading to the death of many kinds of vegetation and decrease of VFC. In without rainy months, temperature and evaporation will be increased, which can adversely affect the normal function of photosynthesis of plants, resulting in reduced VFC. The result showed that CNLI is normally correlated with population and CO_2 emission (Ton/Year), and indicates that urbanization and industrialization keep pace with population growth and CO_2 emission (Ton/Year). Population is significantly correlated with CO_2 emission (Ton/Year) additionally.

Finally, VFC is moderately related to CNLI indicates that on a comprehensive scale over research period of about 16 years, the process of human activities such as urbanization and industrialization had impact on the change of average annual VFC.

5. Conclusions

Accordingly a quantitative research for the 16-year variation of VFC in Iran, using Modis NDVI images, DMSP/OLS datasets and meteorological data from 2000 to 2015, and by dynamically predicting the variation, the conclusion is as follows:

1) The results of the time series analysis of VFC have shown among sixteen research years, the average value of VFC was 14.07%. However, the VFC in 2003 and 2006 have been equal to the average value, and while the VFC in 2000, 2001, 2002, 2008, 2011 and 2012 were less than the average value and subsequently the VFC in 2003, 2004, 2005, 2006, 2009 and 2013 were more than the average value. Mentioned fluctuations in the amount of VFC were derived from climatic factors such as precipitation, evaporation, mean of temperature, mean of rainfall and etc, and also due to increase population and urbanization as well as expanded CNLI and CO_2 emission annually.

2) Spatial distribution of VFC indicated that the oasis is mostly occupied by low (<10%) and very high (>70%) classes, caused by human disturbance such as urbanization, industrialization and land use-land cover change, and also environmental and climatic factors likewise drought were decreased during the four periods of 2000, 2005, 2010 and 2015. On the other side, in the west, northwest and northeast parts of the study area; the economy was unexploited and resulting in the medium class (10-40%) and high class (40-70%) we were dramatically observed rising trend, even thought agricultural and forest improvement activities and climatic factors has been effective undoubtedly.

3) CNLI was greatly indicated human activities. Urbanization and land use-land cover change have expanded form coastal strip of the Caspian Sea and its delta region (Hyrcanian) into inner part of the Iran. Mentioned process is visible in the west and southwest parts. The overall, VFC was related to CNLI indicates on a comprehensive scale, and the dynamic of urbanization and industrialization had a moderate impact on the change of average annual VFC.

4) Temporal dynamic of VFC at the wide scale is largely influence by the fluctuation of climate factors, especially mean of temperature and mean of rainfall annually, which helps to increase VFC and makes many crops, or which decrease of VFC and causes land cover is dried. VFC is positively correlated with mean of temperature and mean of rainfall; however VFC is rarely correlated with CO_2 emissions. Numbers of sunny days (sunshine hours) had very weak correlated with compounded night light index. The reason lies in the fact that both industrialization and urbanization could cause serious air pollution, such as haze, making sunshine hour be decreased.

5) Consequently, the results showed that the by reducing VFC from 1.34% to 1.29%, VFC had significantly fluctuated in Iran from 2000 to 2015. The average value of VFC was raised from 41.74% to 53.13%, 1.37% to 2.25%, and from 1.34% to 1.34 in medium, high and very high classes, and was decreased from 55.52% to 43.24% in low class mutually. Considering the importance of VFC, for the conservation and sustainable development of the ecological environment, for further studies will be the focus on VFC research in the future.

Acknowledgements

The valuable suggestions made by anonymous referees are gratefully acknowledged.

References

[1] Amaral, S., Monteiro, A. M. V., Camara, G and Quintanilha, J. A. 2006. DMSP/OLS nigh-time light imagery for urban population estimates in the Brazilian Amazon. *International Journal of Remote Sensing*. 27 (5): 885-870. DOI: 10.1080/01431160500181861.

[2] Asner, G. P., D. B. Lobell. 2000. A biogeophysical approach for automated SWIR unmixing of soils and vegetation. *Remote Sens. Environ.* 74 (1): 99-112. DOI: 10.1016/S0034-4257(00)00126-7.

[3] Burgess, R., Hansen, M., Olken, B. A., Potapov, P and Sieber, S. 2012. The political economy by multi-temporal classification across the Landsat-5 record. *Remote Sensing of Environment.* 128: 246-258. http://hdl.handle.net/1721.1/82894.

[4] Chand, T. R. K., Badarinath, K. V. S and Prasad, V. K. 2006. Monitoring forest fires over the Indian region using Defence Meteorological Satellite Program-Operational Linescan System nighttime satellite data. *Remote Sensing of Environment.* 103: 165-178.

[5] http://dx.doi.org/10.1016/j.rse.2006.03.010.

[6] Chen, Y. H., Li, X. B., Shi, P. J and Zhou, H. L. 2001. Estimating vegetation fractional coverage using remote sensing data in Haidian District, Beijing. *Acta Phytoecol Sin.* 25: 588-593. DOI: 10.11686/cyxb20140401.

[7] Climate Change Knowledge Portal (CCKP). http://sdwebx.worldbank.org/climateportal.html.

[8] Colombo, R., Bellingeri, D., Fasolini, D and Marino, C. M. 2003. Retrieval of leaf area index in different vegetation types using high resolution satellite data. *Remote Sens. Environ.* 86: 120-131. DOI: 10.1016/S0034-4257(03)00094-4.

[9] Defense Meteorological Satellite Program (DMSP).

[10] https://www.ngdc.noaa.gov/eog/re_direct.html

[11] Elvidge, C. D., Ziskin, D., Baugh, K. E., Tuttle, B. T., Ghosh, T., Pack, D. W., Erwin, E. H., Zhizhin, M., 2009. A fifteen year record of global natural gas flaring derived from satellite data. *Energies.* 2: 595-622. http://dx.doi.org/10.3390/en20300595.

[12] Estel, S., Kuemmerle, T., 2015. Mapping farmland abandonment and recultivation across Europe using MODIS NDVI time series. *Remote Sensing and Environment.* 163: 312-325. http://dx.doi.org/10.1016/j.rse.2015.03.028.

[13] Guan, D., Wang, G and Peart, M. R. 2013. Ecosystem carbon stocks of mangrove forest in Yinglio Bay, Guangdong province of south China. *Forest Ecology and Management*. 310: 539-546. http://dx.doi.org/10.1016/j.foreco.2013.08.045.

[14] Hao, C. Y., LI, X. B., Shi, P. J and Chen, J. 2003. Detecting vegetation fractional coverage of typical steppe in northern china based on multi-scale remotely sensed data. *Acta Botanica Sinica.* 45 (10): 1146-1156. http://en.cnki.com.cn/Article_en/CJFDTOTAL-ZWXB200310003.htm.

[15] He, C. Y., B, Gao. 2015. Dynamics of Urbanization Levels in China from 1992 to 2012: Perspective from DMSP/OLS Nighttime Light Data. *Remote Sens.* 7: 1721-1735. http://dx.doi.org/10.3390/rs70201721.

[16] Huang, Q., Yang, X and Gao, B. 2014. Application of DMSP/OLS night images; A meta-analysis and a systematic literature review. *Remote Sensing.* 6: 6844-6866. http://www.mdpi.com/2072-4292/6/8/6844.

[17] Hyung, K. D., Sexton, J. O and Noojipady, P. 2014. Global, landsat-based forest-cover change from 1990 to 2000. *Remote Sensing of Environment.* 155: 178-193. http://dx.doi.org/10.1016/j.rse.2014.08.017.

[18] Iran Meteorological Organization. http://www.irimo.ir/

[19] Jiapaer, G. L., Chen, X and Bao, A. M. 2011. A comparison of methods for estimating fractional vegetation cover in arid regions. *Agricultural and Forest Meteorology.* 151 (12): 1698-1710. DOI: 10.1007/s40333-013-0145-3.

[20] Ju. W., Zhujun, G., Li, L. 2013. Using vegetation indices and texture measures to estimate vegetation fractional coverage (VFC) of planted and natural forests in Nanjing city, China. *Advances in Space Research*. 51: 1186-1194. http://dx.doi.org/10.1016/j.asr.2012.11.015.

[21] Kenneth, M., Timothy, M., Lynn, F., 2000. Hyperspectral mixture modeling for quantifying sparse vegetation cover in arid environment. *Remote Sens Environ*. 72: 360-374. DOI: 10.1016/S0034-4257(99)00112-1.

[22] Kharol, Sh. K., Badarinath, K. V. S., P. S. Roy., 2008. Studies on emissions from forest fires using multi-satellite datasets over north east region of India. *The international archives of the society for photogrammetry and remote sensing*. ISPRS Archives. Volume XXXVII, Part B8. http://www.isprs.org/proceedings/XXXVII/congress/tc8.aspx.

[23] Kouchi, H. S., M. R. Sahebi., 2013. Fractional vegetation cover estimation in urban environments. *International Archives of the Photogrammetry, Remote Sensing and Spatial Information Sciences*. Volume XL-1/W3, 2013.

[24] http://dx.doi.org/10.5194/isprsarchives-XL-1-W3-357-2013

[25] Li, H., Lu, Z. L and Li, D. Z. 2009. Estimation and monitoring of vegetation coverage dynamics in Chongming county of Shanghai by RS method. *Urban Environment & Urban Ecology*. 22 (2): 8-11.

[26] Liu, J., Yin, S., Zhang, G. S., and et al. 2009. Dynamic change of vegetationcoverage of Mu Us sandland over the 17 years by remote sensingmonitor. *Journal of Arid Land Resources and Environment*. 23 (7): 162-167.

[27] Lucht, W., Coauthors. 2002. Climatic control of the high-latitude vegetation greening trend and Pinatubo effect. *Science*. 296: 1687-1689.

[28] https://dx.doi.org/10.1126/science.1071828.

[29] Lyapustin, A., Wang, Y., and et al. 2014. Scientific impact of MODIS C5 calibration degradation and C6C improvements. *Atmos. Meas. Tech*. 7: 4353-4365. DOI: 10.5194/amt-7-4353-2014.

[30] Moderate Resolution Imaging Spectroradiometer. http://modis.gsfc.nasa.gov/

[31] Nasa earth ovservation. http://neo.sci.gsfc.nasa.gov/

[32] Potapov, P. V., Turubanova, S. A and Tyukavina, A. 2015. Eastern Europe’s forest cover dynamic from 1985 to 2012 quantified from the full Landsat archive. *Remote Sensing of Environment.* 159: 28-43. http://dx.doi.org/10.1016/j.rse.2014.11.027.

[33] Potter, C., S. Boriah., M. Steinbach., V. Kumar., and S. Klooster. 2008. Terrestrial vegetation dynamics and global climate controls. *Climate Dyn.* 31: 67-78. DOI: 10.1007/s00382-007-0339-5.

[34] Schneider, A., Friedl, M. A and Potere, D. 2009. A new map of global urban extent from MODIS satellite data. *Environmental Research Letters*. 4, 044003. http://dx.doi.org/10.1088/1748-9326/4/4/044003.

[35] Sexton, J. O., Urban, D. L., Donohue, M. J and Song, C. 2013. Long-term land cover dynamics of deforestation in the tropics. *Quarterly Journal of Economics*. 127 (4): 1707-1754. http://www.oalib.com/references/19828259.

[36] Small, C., Pozzi, F and C. D. Elvidge. 2005. Spatial analysis of global urban extent from DMSP-OLS night lights. *Remote Sensing of Environment*. 96: 277-291. http://dx.doi.org/10.1016/j.rse.2005.02.002.

[37] Wu, B. F., Fei. L., and et al. 2014. Improving Estimates of Grassland Fractional Vegetation Cover Based on a Pixel Dichotomy Model: A Case Study in Inner Mongolia. China. *Remote Sens.* 6: 4705-4722. http://dx.doi.org/10.3390/rs6064705.

[38] Yang, G. H., Bao, A. M., Chen, X., 2010. Vegetation cover change with climate and land use variation along main stream of Tarim River. *Journal of Desert Research*. 30 (6), 1389-1397. http://en.cnki.com.cn/Article_en/CJFDTotal-ZGSS201006024.htm.

[39] Zhang, F., Tiyip, T and Ding, J. L. 2013. Vegetation fractional coverage change in a typical oasis region in Tarim river watershed based on remote sensing. *Journal of Arid Land*. 5 (1): 89-101. doi: 10.1007/s40333-013-0145-3.